



Available online at <http://scik.org>

Commun. Math. Biol. Neurosci. 2023, 2023:70

<https://doi.org/10.28919/cmbn/8027>

ISSN: 2052-2541

MITIGATION OF CLIMATE CHANGE DUE TO EXCESSIVE CARBON DIOXIDE EMISSION AND ACCUMULATION: A MATHEMATICAL MODEL APPROACH

PETER URANE ACHIMUGWU^{1,*}, MATHEW NGUGI KINYANJUI², DAVID MUMO MALONZA³

¹Pan African University Institute for Basic Sciences, Technology and Innovation, Nairobi, Kenya

²School of Pure and Applied Mathematics, Jomo Kenyatta University of Agriculture and Technology, Juja, Kenya

³Department of Mathematics and Actuarial Science, South Eastern Kenya University, Kitui, Kenya

Copyright © 2023 the author(s). This is an open access article distributed under the Creative Commons Attribution License, which permits unrestricted use, distribution, and reproduction in any medium, provided the original work is properly cited.

Abstract. One of the current phenomena causing a global emergency is climate change. This change is attributed to various human activities that release greenhouse gases in great amount into our environment. The most crucial and abundant of these gases is carbon dioxide. Excessive emission and accumulation of this gas has negatively affected various sectors of life. Some of the consequences of this climate change as result of excessive emission and accumulation of carbon dioxide are flooding, drought, wildlife migration, disease outbreak, to mention but a few. This research study proposes a deterministic compartmental model of mitigating against excessive emission and accumulation of carbon dioxide into the atmosphere. Hence, we considered dynamics involving the following variables: photosynthetic biomass density, good conservation policies, enlightenment programmes, as well as direct air capture technology. Based on the model assumptions, the model equations of five compartments were formulated. A threshold quantity analogous to other quantities like the Basic Reproduction, Consumption Number, Predation Number, called the Concentration Number that determines the danger of excessive concentration of carbon dioxide in the atmosphere was obtained using the idea of Next Generation Matrix. Local stability analysis of the equilibrium points obtained was carried out. Furthermore, the sensitivity analysis was done using the Concentration Number and through this, key parameters that influence the dynamics of the model were identified. Finally, numerical simulations were done to find out the effect of each mitigation measure and their combinations

*Corresponding author

E-mail address: peter.achimugwu@students.jkuat.ac.ke

Received May 19, 2023

in reducing the excess accumulated concentration of carbon dioxide in the atmosphere. From the findings, combining effectively mitigation measures such as good conservation policies, enlightenment programmes and direct air capture technology with an improved photosynthetic biomass density would greatly reduce the excess accumulated concentration of carbon dioxide from the atmosphere.

Keywords: mitigation of climate change; greenhouse gases; excessive carbon dioxide; mathematical model; concentration number; equilibrium points; local stability.

2020 AMS Subject Classification: 86A08.

NOMENCLATURE

TABLE 1. **Descriptions of Model Variables and Parameters**

Symbols	Descriptions
t	Time
$C(t)$	Excessive concentration of CO_2 in the atmosphere
$P(t)$	Photosynthetic biomass density
$R(t)$	Good conservation policies density
$E(t)$	Enlightenment programmes density
$T(t)$	Direct air capture technology density
β	Intrinsic rate of accumulation of CO_2 in the atmosphere
C_m	Maximum tolerated concentration of CO_2 beyond which the model becomes meaningless
d_1	Rate of decrease in CO_2 concentration due to interaction between CO_2 and the photosynthetic biomass
d_2	Rate of decrease in CO_2 concentration due to implementation of good conservation policies
d_3	Rate of decrease in CO_2 concentration due to implementation of enlightenment programmes
d_4	Rate of decrease in CO_2 concentration due to implementation of direct air capture technology
μ_0	Natural rate of depletion in concentration of CO_2
ω	Intrinsic rate of growth of the photosynthetic biomass
N	Carrying capacity for the photosynthetic biomass
ϕ	Rate of increase in the photosynthetic biomass due to the interaction between this biomass and CO_2 (photosynthetic rate)
τ	Rate of increase in photosynthetic biomass due to interaction between good conservation policies and the photosynthetic biomass
μ_1	Rate of decrease in photosynthetic biomass due to natural phenomena
μ_2	Rate of decrease in photosynthetic biomass due to human activities
a_1	Rate of success of good conservation policies
a_0	Rate of negligence or evasion of good conservation policies
b_1	Rate of success of enlightenment programmes
b_0	Rate of Ignorance, negligence and evasion of the enlightenment programmes
m_1	Rate of success of direct air capture technology
m_0	Rate of decline in the implementation of direct air capture technology

1. INTRODUCTION

The global community is currently plagued with many environmental challenges. Most of these problems have been attributed to global climate change arising from over exploitation of our planet. Climate change is caused by excessive emission and accumulation of greenhouse gases into our environment. The most crucial contributor of all these gases to the current narrative of climate change issue is carbon dioxide. Excessive emission of this gas into our environment raises the global temperature beyond optimal level and the attendant consequences of this are manifested through various natural disasters such as aridity, flooding, drought, and many others. Human activities such as agriculture, industrialization, urbanization, deforestation, transportation, mining, electricity generation have contributed greatly to the excessive emission of the greenhouse gases, especially carbon dioxide into our environment. The devastating effect of climate change is felt by almost every country in the world. There is growing concern about climate change because of the rise in average global temperature. This has been attributed greatly to excessive emission and accumulation of greenhouse gases. Civilization and anthropogenic activities have prompted the hazards of global warming, climate change and bad impacts on our quality of life [1].

Six greenhouse gases are covered under the Kyoto Protocol. Carbon dioxide makes up the greatest part of greenhouse gas emissions and has become the most vital anthropogenic greenhouse gas. The greatest contributions to GHG emissions are from the electricity and petroleum industries, followed by the transportation sector and other industries. Decision makers formulate practicable and sustainable environmental policies, regulate energy structure of industrial production, and efficiently decrease carbon emissions and help in achieving a country's environmental stability through accurate carbon dioxide forecasting [2]. According to the National Plan for Adaption to Climate Change (NPACC), South America risks losing 23% of its species as a consequence of climate warming [3]. Brazil as the fifth largest country in the global geography, made a commitment under the Paris Agreement, that by 2025, greenhouse gases emissions would be at 37% and that by 2020, carbon dioxide emission will be around 43% [3]. [4] noted that there was a rise in temperature of water due to excessive emission of greenhouse gases, which consequently led to a decrease in the level of dissolved oxygen and also a rise in the rate

of circulation of disintegrated oxygen by aquatic inhabitants, thereby leading to a decline in the density of these aquatic animals.

Different mathematical models on climate change have been developed by considering effects of one or two of deforestation, human population, population pressure, migration, urbanization, industrialization, awareness, to mention but a few. [5] in studying the problem of global warming due to increasing emission of greenhouse gases, 83% of which were from different human activities and the remaining 17% being from wild animals, developed and analyzed a four compartment mathematical model. Their findings revealed that human beings were solely responsible for the current increased emission of the greenhouse gases and global warming, and the attendant consequences of this was felt by both the human community and the forest ecosystem. [6] studied and investigated a mathematical model applied to green building concept for sustainable cities under climate change. From their analyses, they found out that: global warming was increasing at an alarming rate due to extreme emission of greenhouse gases. [7] formulated a non-linear mathematical model by considering forest biomass and global warming as separate compartments. The results obtained from his analysis showed that increase in the area of forest biomass led to a reduction in global warming and increased rate of harvesting of forest biomass led to increase in global warming. [8] developed a model on the reduction of CO_2 emission by optimally tracking a pre-defined target. Their findings revealed that the emission target could be achieved by 2014 with investments in reforestation; a reduction of the expected GDP of 42% relative to 2006; increase in clean technology between 2008 and 2010 due to investment of maximum figures of about 70 million USD; and a relatively high cumulative costs depending on the price of carbon abatement and the rate at which the expected CO_2 concentration in the atmosphere should be reduced. [9] developed a nonlinear mathematical model to study the effect of reforestation as well as the delay encountered between the measurement of forest data and implementation of reforestation efforts on the control of atmospheric concentration of carbon dioxide. From their analysis, concentration of atmospheric carbon dioxide decreased due to reforestation. [10] developed an ecological type nonlinear mathematical model for the removal of carbon dioxide from the regional atmosphere by externally introduced liquid species, which could react with this gas and remove it by gravity. He showed analytically and numerically that

the concentration of carbon dioxide decreased as the rate of introduction of externally introduced liquid species increased. [11] developed a simplified mathematical model to study the effect of carbon dioxide on the mechanism of global warming by considering emissivity of the gases (water vapour and carbon dioxide) to be dependent on three variables which were temperature, gas concentration and beam length of the atmospheric layer defined through the model. Their findings revealed that the temperature of the Earth rose enormously with CO_2 concentration. [12] provided an accessible mathematical approach used to design models that show smooth patterns of global carbon dioxide emissions which are in agreement with the UN climate targets. His findings through appropriate interpolations showed that the smooth pathways would overcome a global lack of no-carbon energy in the short run and tolerate low emissions that could disappear as adequately required from 2040s with the direct removal of CO_2 becoming immaterial in the long run. [13] used optimal control theory to obtain effective and useful distribution of investments in reforestation and encouragement of certain technology to attain a carbon dioxide emission schedule for 2020 in the Legal Brazilian Amazon (BA). Their simulation results showed that a forest area of about $3.7 \times 10^6 \text{ km}^2$ was needed for CO_2 emission target of 3.76×10^8 tonnes in 2020, which could require about $4.5 \times 10^5 \text{ km}^2$ reforestation out of this total land area. [14] in studying the grave problem of climate change caused by rise in the mean global temperature resulting from excessive emission of greenhouse gases, especially carbon dioxide, developed a nonlinear mathematical model made up of five compartments. Their results revealed that the concentration of CO_2 reduced as the rates of spray of liquid phase and solid particulate matters increase in the atmosphere and could be eliminated, if the rates of the spray of the external species were very large. In trying to reduce carbon dioxide emissions through carbon capture and storage in a saline aquifer, [15] developed and analyzed simple mathematical models for the trapping processes of CO_2 . His findings revealed that the emission of CO_2 can be greatly reduced using saline aquifer. [16] developed a mathematical model for removing carbon dioxide from the atmosphere by the introduction of external species which reacts with the CO_2 to render it harmless and also through plantation of leafy greenbelts (which also removes the CO_2 gas through the natural process of photosynthesis). From their findings from both the analytical and numerical simulation, as the rate of introduction of external species

increased, the concentration of carbon dioxide decreased. Similarly, as the rate of absorption of carbon dioxide by greenbelts became very large, the concentration of carbon dioxide also reduced. [17] developed and analyzed a nonlinear mathematical model to study deforestation of forest resources due to lack of clear information about utilities of the forest and increasing forestry resources by plantation on the conservation of forestry resources. From their analytical and numerical results, the cumulative density of forest resources decreased as the density of population and population pressure increased. Furthermore, awareness of human population on the importance of forest resources decreased deforestation activities. [18] investigated how to control global warming caused by carbon dioxide by considering two models. They showed analytically and numerically, that the concentration of carbon dioxide decreased as the concentration of externally introduced liquid species increased and if the rate of introduction of liquid is very high, carbon dioxide would be removed totally from the atmosphere. [19] developed a four-compartment nonlinear ordinary differential equations containing a wide number of model parameters that affect climate due to emission of carbon dioxide. Their findings revealed that the most sensitive parameters in the model were the concentration of a suitable absorbent and the rate of inflow of absorbent in the absorption chamber.

In the study we are proposing to undertake, we shall narrow our focus on three lead papers. [17], [18], and [19] developed mathematical models by considering the effects of externally introduced liquid species; externally introduced liquid species and plant biomass density; and awareness of human population respectively, on reduction of consequences of global warming. No single mitigation measure is enough to combat the dangers posed by climate change. Therefore, we need a combination of mitigation measures to produce a better result. Hence, we propose to incorporate photosynthetic biomass density, good conservation policies, enlightenment programmes, and direct air capture technology in the model dynamics of reducing the excessive concentration of carbon dioxide emission and accumulation into the atmosphere.

2. MODEL FORMULATION

The following assumptions were made in the formulation of the model:

- i. All parameters and variables involved in the model are non-negative since the system under consideration is biological;
- ii. Excessive emission and accumulation of carbon dioxide, a greenhouse gas, into the atmosphere is solely responsible for current climate change;
- iii. The concentration of carbon dioxide in the atmosphere constantly increases due to human activities such as rapid increase in industrialization, excessive combustion of fossil fuels, urbanization, deforestation, modern lifestyles, to mention but a few;
- iv. There is a threshold concentration level (maximum tolerant level) of carbon dioxide beyond which the model becomes irrelevant;
- v. The effect of climate change arising from excessive emission and accumulation of carbon dioxide into the atmosphere will be under check by incorporating some mitigation measures;
- vi. The emission and accumulation of carbon dioxide follows a form of logistic growth model pattern;
- vii. The growth of the photosynthetic biomass density also follows a logistic growth pattern;
- viii. Photosynthetic biomass density can be increased through plantation, afforestation, seed dispersal and pollination;
- ix. The rate of incorporation of each mitigation measure is directly proportional to the concentration of carbon dioxide;
- x. Awareness of the hazards of excessive concentration of carbon dioxide in the atmosphere and the relevance of discouraging deforestation activities as well as encouraging good conservation policies would contribute to a reduction of excessive emission of carbon dioxide into the atmosphere.

The variables considered in this model are: Excessive concentration of carbon dioxide, $C(t)$; Photosynthetic biomass density, $P(t)$; Good conservation policies density, $R(t)$; Enlightenment programmes density, $E(t)$ and Direct air capture technology density, $T(t)$. The intrinsic rate of

accumulation of carbon dioxide in the atmosphere is denoted by β and the term $\beta C \left(1 - \frac{C}{C_m}\right)$ represents the cumulative accumulation of carbon dioxide in the atmosphere, where C_m represents the maximum tolerated concentration of CO_2 beyond which the model becomes non-meaningful. Due to the interaction between carbon dioxide in the atmosphere and the photosynthetic biomass, the concentration of CO_2 reduces at a rate of d_1 . In trying to mitigate against excessive emission of this gas, d_2 represents rate of reduction of the gas from implementation of good conservation policies, d_3 represents rate of reduction of concentration of CO_2 in the atmosphere due to success of the enlightenment programmes and d_4 represents the rate of reduction in concentration of CO_2 due to use of technology that could capture this gas and convert it to a less harmful substance or even store it for other use. Finally, μ_0 represents the natural rate of depletion in concentration of CO_2 in the atmosphere. The intrinsic rate of growth of the photosynthetic biomass is denoted by ω and the cumulative growth of this photosynthetic biomass is assumed to follow a logistic growth pattern as seen in the term $\omega P \left(1 - \frac{P}{N}\right)$, where N is the carrying capacity for this photosynthetic biomass. Effective awareness programmes lead to people engaging in good conservation policies such as reforestation, afforestation, avoidance of bush burning, reclaiming of desert lands through some modern methods and many others. This in turn is assumed to contribute to the growth of the photosynthetic biomass density at a rate of τ . μ_1 represents the rate of decrease in photosynthetic biomass density due to natural phenomena such as wildfires, disease outbreak, flooding, drought, overgrazing and many more. There is also a decrease in this biomass due to human activities such as cutting down of forests for food, shelter, industrialization, urbanization, woods, honey, different medicinal products and many others. This could also be referred to as the artificial depletion in the photosynthetic biomass density and this occurs at a rate of μ_2 .

In the third equation, we assumed that the rate of implementation of good conservation policies is directly proportional to the concentration of CO_2 in the atmosphere and hence, the reason for the term $a_1 C$, where a_1 is the rate of reduction of carbon dioxide due to good conservation policies. Due to positive impact of enlightenment, we assumed there is an improvement in good conservation policies and knowledge about the dangers of unchecked emission of carbon dioxide. Negligence or evasion of good conservation policies is assumed to occur at rate of

a_0 . Same analogy goes for the fourth and fifth equations. Hence, the deterministic nonlinear compartmental climate model equations are:

$$(1) \quad \frac{dC}{dt} = \beta C \left(1 - \frac{C}{C_m}\right) - d_1 CP - (d_2 + d_3 + d_4 + \mu_0)C,$$

$$(2) \quad \frac{dP}{dt} = \omega P \left(1 - \frac{P}{N}\right) + \phi CP + \tau PR - (\mu_1 + \mu_2)P,$$

$$(3) \quad \frac{dR}{dt} = a_1 C - a_0 R,$$

$$(4) \quad \frac{dE}{dt} = b_1 C - b_0 E,$$

$$(5) \quad \frac{dT}{dt} = m_1 C - m_0 T,$$

subject to the non-negative initial conditions:

$$C(t) = C_0, P(t) = P_0, R(t) = R_0, E(t) = E_0, T(t) = T_0.$$

In our formulation, it is assumed that the functions $C(t), P(t), R(t), E(t), T(t)$ and their corresponding derivatives are continuous at $t \geq 0$ for $0 < C(t) \leq C_m, 0 < P(t) \leq N, R(t) > 0, E(t) > 0, T(t) > 0$.

3. MATHEMATICAL ANALYSIS

3.1. Concentration Number. Using the analogy of the basic reproduction number, R_0 , in epidemiological mathematical models [20], [21], [22]; predation number, P_0 , in prey-predator relationship mathematical model [23]; consumption number, C_0 , as also used in ecological models [24], [25], [26], [27], which are all using the idea of the Next Generation matrix [20], we have come up with a similar threshold quantity which we call *Concentration Number*, C_* .

The concentration number, C_* , is a threshold quantity that determines how dangerous the concentration of CO_2 is in the atmosphere. If $C_* < 1$, then the emission and accumulation of CO_2 is not harmful to the ecosystem. However, if $C_* > 1$, then we have excessive emission and accumulation of CO_2 in the atmosphere which could lead to climate change as time evolves and hence, mitigation measures have to be put in place to check this excessive emission. To get the concentration number, we split the model equations to form two matrices F_i and V_i respectively. F_i matrix contains interaction terms of the model equations while V_i contains a negation of the non-interactive terms of the model equations. The matrix got from F_i is denoted F while the

one got from V_i is denoted V . C_* is the spectral radius of the next generation matrix, FV^{-1} . That is,

$$(6) \quad C_* = \rho(FV^{-1}).$$

We obtain the mathematical expression for concentration number, C_* , as follows:

Let

$$C \neq 0, P = 0, R = 0, E = 0, T = 0.$$

Considering equation (1) at equilibrium;

$$(7) \quad C = \frac{C_m[\beta - (d_2 + d_3 + d_4 + \mu_0)]}{\beta}, \beta > (d_2 + d_3 + d_4 + \mu_0).$$

Therefore, the required point for obtaining the Concentration Number is thus:

$$(8) \quad (C, P, R, E, T) = \left(\frac{C_m[\beta - (d_2 + d_3 + d_4 + \mu_0)]}{\beta}, 0, 0, 0, 0 \right), \beta > (d_2 + d_3 + d_4 + \mu_0).$$

P, R, E and T are zero because it is assumed that at this point, there is no mitigation measure so that we would be able to find out if there is excessive emission or not.

Obtaining matrices F_i and V_i , we have:

$$(9) \quad F_i = \begin{pmatrix} F_1 \\ F_2 \\ F_3 \\ F_4 \\ F_5 \end{pmatrix} = \begin{pmatrix} -d_1CP \\ \phi CP + \tau PR \\ 0 \\ 0 \\ 0 \end{pmatrix}.$$

$$(10) \quad V_i = \begin{pmatrix} V_1 \\ V_2 \\ V_3 \\ V_4 \\ V_5 \end{pmatrix} = \begin{pmatrix} -\beta C \left(1 - \frac{C}{C_m} \right) + (d_2 + d_3 + d_4 + \mu_0)C \\ -\omega P \left(1 - \frac{P}{N} \right) + (\mu_1 + \mu_2)P \\ -a_1C + a_0R \\ -b_1C + b_0E \\ -m_1C + m_0T \end{pmatrix}.$$

The matrices F and V are obtained by evaluating the Jacobian matrices of F_i and V_i at the point given by equation (8) as follows:

$$(11) \quad F = \begin{pmatrix} 0 & -\frac{C_m d_1 [\beta - (d_2 + d_3 + d_4 + \mu_0)]}{\beta} & 0 & 0 & 0 \\ 0 & \frac{C_m \phi [\beta - (d_2 + d_3 + d_4 + \mu_0)]}{\beta} & 0 & 0 & 0 \\ 0 & 0 & 0 & 0 & 0 \\ 0 & 0 & 0 & 0 & 0 \\ 0 & 0 & 0 & 0 & 0 \end{pmatrix}.$$

$$(12) \quad V = \begin{pmatrix} [\beta - (d_2 + d_3 + d_4 + \mu_0)] & 0 & 0 & 0 & 0 \\ 0 & [-\omega + (\mu_1 + \mu_2)] & 0 & 0 & 0 \\ -a_1 & 0 & a_0 & 0 & 0 \\ -b_1 & 0 & 0 & b_0 & 0 \\ -m_1 & 0 & 0 & 0 & m_0 \end{pmatrix}.$$

By evaluation, we have:

$$(13) \quad V^{-1} = \begin{pmatrix} \frac{1}{[\beta - (d_2 + d_3 + d_4 + \mu_0)]} & 0 & 0 & 0 & 0 \\ 0 & \frac{1}{[-\omega + (\mu_1 + \mu_2)]} & 0 & 0 & 0 \\ \frac{a_1}{a_0} & 0 & \frac{1}{a_0} & 0 & 0 \\ \frac{b_1}{b_0} & 0 & 0 & \frac{1}{b_0} & 0 \\ \frac{m_1}{m_0} & 0 & 0 & 0 & \frac{1}{m_0} \end{pmatrix}.$$

The next generation matrix (NGM), FV^{-1} , is determined using equations (8) and (13) and the result is given thus:

$$(14) \quad \therefore FV^{-1} = \begin{pmatrix} 0 & -\frac{C_m d_1 [\beta - (d_2 + d_3 + d_4 + \mu_0)]}{\beta [-\omega + (\mu_1 + \mu_2)]} & 0 & 0 & 0 \\ 0 & \frac{\phi C_m [\beta - (d_2 + d_3 + d_4 + \mu_0)]}{\beta [-\omega + (\mu_1 + \mu_2)]} & 0 & 0 & 0 \\ 0 & 0 & 0 & 0 & 0 \\ 0 & 0 & 0 & 0 & 0 \\ 0 & 0 & 0 & 0 & 0 \end{pmatrix}.$$

The characteristic equation corresponding to FV^{-1} is:

$$\begin{vmatrix} -\lambda & -\frac{C_m d_1 [\beta - (d_2 + d_3 + d_4 + \mu_0)]}{\beta [-\omega + (\mu_1 + \mu_2)]} & 0 & 0 & 0 \\ 0 & \frac{\phi C_m [\beta - (d_2 + d_3 + d_4 + \mu_0)]}{\beta [-\omega + (\mu_1 + \mu_2)]} - \lambda & 0 & 0 & 0 \\ 0 & 0 & -\lambda & 0 & 0 \\ 0 & 0 & 0 & -\lambda & 0 \\ 0 & 0 & 0 & 0 & -\lambda \end{vmatrix} = 0.$$

From the above, the eigenvalues of FV^{-1} are:

$$\lambda_1 = 0; \lambda_2 = \frac{\phi C_m [\beta - (d_2 + d_3 + d_4 + \mu_0)]}{\beta [-\omega + (\mu_1 + \mu_2)]} \equiv -\frac{\phi C_m [\beta - (d_2 + d_3 + d_4 + \mu_0)]}{\beta [\omega - (\mu_1 + \mu_2)]}; \lambda_3 = 0;$$

$$\lambda_4 = 0; \lambda_5 = 0.$$

The concentration number, C_* is thus the spectral radius of FV^{-1} . That is,

$$(15) \quad C_* = \rho(FV^{-1}) = \max |\lambda_1, \lambda_2, \lambda_3, \lambda_4, \lambda_5|.$$

Considering the above eigenvalues, the concentration number which is equivalent to the maximum eigenvalue is

$$(16) \quad C_* = \frac{\phi C_m [\beta - (d_2 + d_3 + d_4 + \mu_0)]}{\beta [\omega - (\mu_1 + \mu_2)]}; \beta > (d_2 + d_3 + d_4 + \mu_0), \omega > (\mu_1 + \mu_2).$$

3.2. Equilibrium Points. The equilibrium points of the model system given by equations (1), (2), (3), (4) and (5) can be obtained by equating each of these equations to zero and solving for the dependent variables. That is;

$$\frac{dC}{dt} = 0, \frac{dP}{dt} = 0, \frac{dR}{dt} = 0, \frac{dE}{dt} = 0, \frac{dT}{dt} = 0.$$

A summary of the four equilibrium points obtained are:

$$\varepsilon_0 = (C^0, P^0, R^0, E^0, T^0) = (0, 0, 0, 0, 0).$$

$$\varepsilon_1 = (C^*, P^*, R^*, E^*, T^*).$$

$$\varepsilon_2 = (C^{**}, P^{**}, R^{**}, E^{**}, T^{**}) = \left(0, \frac{N}{\omega} [\omega - (\mu_1 + \mu_2)], 0, 0, 0 \right).$$

$$\varepsilon_3 = (C^{***}, P^{***}, R^{***}, E^{***}, T^{***}).$$

Where,

$$C^* = \frac{C_m}{\beta} [\beta - (d_2 + d_3 + d_4 + \mu_0)], \beta > (d_2 + d_3 + d_4 + \mu_0).$$

$$P^* = 0.$$

$$R^* = \frac{a_1 C_m}{a_0 \beta} [\beta - (d_2 + d_3 + d_4 + \mu_0)], \beta > (d_2 + d_3 + d_4 + \mu_0).$$

$$E^* = \frac{b_1 C_m}{b_0 \beta} [\beta - (d_2 + d_3 + d_4 + \mu_0)], \beta > (d_2 + d_3 + d_4 + \mu_0).$$

$$T^* = \frac{m_1 C_m}{m_0 \beta} [\beta - (d_2 + d_3 + d_4 + \mu_0)], \beta > (d_2 + d_3 + d_4 + \mu_0).$$

$$C^{***} = \frac{a_0 \beta C_m \omega - a_0 C_m \{d_1 N [\omega - (\mu_1 + \mu_2)] + \omega (d_2 + d_3 + d_4 + \mu_0)\}}{a_0 \beta \omega + C_m d_1 N (a_0 \phi + \tau a_1)},$$

$$a_0 \beta C_m \omega > a_0 C_m \{d_1 N [\omega - (\mu_1 + \mu_2)] + \omega (d_2 + d_3 + d_4 + \mu_0)\}.$$

$$P^{***} = N \left[\frac{C_m (a_0 \phi + \tau a_1) [\beta - (d_2 + d_3 + d_4 + \mu_0)] + a_0 \beta [\omega - (\mu_1 + \mu_2)]}{a_0 \beta \omega + C_m d_1 N (a_0 \phi + \tau a_1)} \right],$$

$$\beta > (d_2 + d_3 + d_4 + \mu_0).$$

$$R^{***} = \frac{a_1}{a_0} C^{***} = a_1 \left[\frac{\beta C_m \omega - C_m \{d_1 N [\omega - (\mu_1 + \mu_2)] + \omega (d_2 + d_3 + d_4 + \mu_0)\}}{a_0 \beta \omega + C_m d_1 N (a_0 \phi + \tau a_1)} \right].$$

$$E^{***} = \frac{b_1}{b_0} C^{***} = \frac{b_1}{b_0} \left[\frac{a_0 \beta C_m \omega - a_0 C_m \{d_1 N [\omega - (\mu_1 + \mu_2)] + \omega (d_2 + d_3 + d_4 + \mu_0)\}}{a_0 \beta \omega + C_m d_1 N (a_0 \phi + \tau a_1)} \right].$$

$$T^{***} = \frac{m_1}{m_0} C^{***} = \frac{m_1}{m_0} \left[\frac{a_0 \beta C_m \omega - a_0 C_m \{d_1 N [\omega - (\mu_1 + \mu_2)] + \omega (d_2 + d_3 + d_4 + \mu_0)\}}{a_0 \beta \omega + C_m d_1 N (a_0 \phi + \tau a_1)} \right].$$

3.3. Stability Analysis. To carry out the local stability analysis of the equilibrium points obtained, we linearize the model system given by equations (1) to (5) by generating a Jacobian (characteristic) matrix, J , and then evaluating this matrix at each of the equilibrium points.

The Jacobian matrix, J , is given thus:

$$(17) \quad J = \begin{pmatrix} \beta \left(1 - \frac{2C}{C_m}\right) - d_1 P - (d_2 + d_3 + d_4 + \mu_0) & -d_1 C & 0 & 0 & 0 \\ \phi P & \omega \left(1 - \frac{2P}{N}\right) + \phi C + \tau R - (\mu_1 + \mu_2) & \tau P & 0 & 0 \\ a_1 & 0 & -a_0 & 0 & 0 \\ b_1 & 0 & 0 & -b_0 & 0 \\ m_1 & 0 & 0 & 0 & -m_0 \end{pmatrix}$$

Theorem 3.1. *The equilibrium point $\varepsilon_0 = (C^0, P^0, R^0, E^0, T^0) = (0, 0, 0, 0, 0)$ is locally asymptotically stable if $\beta < (d_2 + d_3 + d_4 + \mu_0)$ and $\omega < \mu_1 + \mu_2$. It is unstable if $\beta > (d_2 + d_3 + d_4 + \mu_0)$ and $\omega > \mu_1 + \mu_2$.*

Proof. At the first equilibrium point (trivial equilibrium point), $\varepsilon_0 = (0, 0, 0, 0, 0)$, we have the Jacobian matrix given by equation (17) as:

$$J_0 = \begin{pmatrix} \beta - (d_2 + d_3 + d_4 + \mu_0) & 0 & 0 & 0 & 0 \\ 0 & \omega - (\mu_1 + \mu_2) & 0 & 0 & 0 \\ a_1 & 0 & -a_0 & 0 & 0 \\ b_1 & 0 & 0 & -b_0 & 0 \\ m_1 & 0 & 0 & 0 & -m_0 \end{pmatrix}$$

The characteristic equation for the Jacobian matrix, J_0 , is given by:

$$|J_0 - \lambda I| = 0$$

$$\Rightarrow \begin{vmatrix} \beta - (d_2 + d_3 + d_4 + \mu_0) - \lambda & 0 & 0 & 0 & 0 \\ 0 & \omega - (\mu_1 + \mu_2) - \lambda & 0 & 0 & 0 \\ a_1 & 0 & -a_0 - \lambda & 0 & 0 \\ b_1 & 0 & 0 & -b_0 - \lambda & 0 \\ m_1 & 0 & 0 & 0 & -m_0 - \lambda \end{vmatrix} = 0$$

Evaluating this determinant, we obtain:

$$\lambda = \beta - (d_2 + d_3 + d_4 + \mu_0), \lambda = \omega - (\mu_1 + \mu_2), \lambda = -a_0, \lambda = -b_0, \lambda = -m_0$$

Since all the parameters are non-negative, then;

$$\lambda_1 = \beta - (d_2 + d_3 + d_4 + \mu_0); \lambda_2 = \omega - (\mu_1 + \mu_2); \lambda_3 = -a_0 < 0; \lambda_4 = -b_0 < 0; \lambda_5 = -m_0 < 0.$$

An equilibrium point is locally asymptotically stable if all the eigenvalues are real and negative. Hence, the stability of the first equilibrium point, $\varepsilon_0 = (0, 0, 0, 0, 0)$, is dependent on the nature of the first,

$\lambda_1 = \beta - (d_2 + d_3 + d_4 + \mu_0)$ and second, $\lambda_2 = \omega - (\mu_1 + \mu_2)$ eigenvalues. We take a look at four cases for the trivial equilibrium point thus:

CASE I: $\lambda_1 > 0$ and $\lambda_2 > 0$.

If $\lambda_1 > 0$, then $\beta > (d_2 + d_3 + d_4 + \mu_0)$ and if $\lambda_2 > 0$, then $\omega > (\mu_1 + \mu_2)$.

These two conditions make the trivial equilibrium point of the model system unstable. Thus, for this case, the equilibrium point $\varepsilon_0 = (C^0, P^0, R^0, E^0, T^0) = (0, 0, 0, 0, 0)$ will be a *source*.

CASE II: $\lambda_1 > 0$ and $\lambda_2 < 0$.

If $\lambda_1 > 0$, then $\beta > (d_2 + d_3 + d_4 + \mu_0)$ and if $\lambda_2 < 0$, then $\omega < (\mu_1 + \mu_2)$.

These conditions make the equilibrium point $\varepsilon_0 = (C^0, P^0, R^0, E^0, T^0) = (0, 0, 0, 0, 0)$ unstable as well. Thus, $\varepsilon_0 = (C^0, P^0, R^0, E^0, T^0) = (0, 0, 0, 0, 0)$ will be a *saddle point*.

CASE III: $\lambda_1 < 0$ and $\lambda_2 > 0$.

If $\lambda_1 < 0$, then $\beta < (d_2 + d_3 + d_4 + \mu_0)$ and if $\lambda_2 > 0$, then $\omega > (\mu_1 + \mu_2)$.

These conditions make the equilibrium point $\varepsilon_0 = (C^0, P^0, R^0, E^0, T^0) = (0, 0, 0, 0, 0)$ unstable also. Thus, $\varepsilon_0 = (C^0, P^0, R^0, E^0, T^0) = (0, 0, 0, 0, 0)$ will be a *saddle point*.

CASE IV: $\lambda_1 < 0$ and $\lambda_2 < 0$.

If $\lambda_1 < 0$, then $\beta < (d_2 + d_3 + d_4 + \mu_0)$ and if $\lambda_2 < 0$, then $\omega < (\mu_1 + \mu_2)$.

These conditions make the equilibrium point $\varepsilon_0 = (C^0, P^0, R^0, E^0, T^0) = (0, 0, 0, 0, 0)$ to be locally asymptotically stable. Thus, $\varepsilon_0 = (C^0, P^0, R^0, E^0, T^0) = (0, 0, 0, 0, 0)$ will be a *sink*. \square

Theorem 3.2. *The equilibrium point $\varepsilon_1 = (C^*, P^*, R^*, E^*, T^*)$ is locally asymptotically stable if $\omega + \left(\phi + \frac{a_1\tau}{a_0}\right)C^* < (\mu_1 + \mu_2)$. It is unstable if $\omega + \left(\phi + \frac{a_1\tau}{a_0}\right)C^* > (\mu_1 + \mu_2)$, where $C^* = \frac{C_m}{\beta} [\beta - (d_2 + d_3 + d_4 + \mu_0)]$, $\beta > (d_2 + d_3 + d_4 + \mu_0)$.*

Proof. The Jacobian matrix, J_1 , of equation (17) evaluated at $\varepsilon_1 = (C^*, P^*, R^*, E^*, T^*)$ is:

$$J_1 = \begin{pmatrix} -\frac{\beta}{C_m}C^* & -d_1C^* & 0 & 0 & 0 \\ 0 & \omega - (\mu_1 + \mu_2) + \left(\phi + \frac{a_1\tau}{a_0}\right)C^* & 0 & 0 & 0 \\ a_1 & 0 & -a_0 & 0 & 0 \\ b_1 & 0 & 0 & -b_0 & 0 \\ m_1 & 0 & 0 & 0 & -m_0 \end{pmatrix}.$$

The corresponding characteristic equation for the above Jacobian matrix, J_1 , is:

$$|J_1 - \lambda I| = \begin{vmatrix} -\frac{\beta}{C_m}C^* - \lambda & -d_1C^* & 0 & 0 & 0 \\ 0 & \omega - (\mu_1 + \mu_2) + \left(\phi + \frac{a_1\tau}{a_0}\right)C^* - \lambda & 0 & 0 & 0 \\ a_1 & 0 & -a_0 - \lambda & 0 & 0 \\ b_1 & 0 & 0 & -b_0 - \lambda & 0 \\ m_1 & 0 & 0 & 0 & -m_0 - \lambda \end{vmatrix} = 0.$$

$$\lambda_1 = -\frac{\beta}{C_m}C^* < 0, \lambda_2 = \omega - (\mu_1 + \mu_2) + \left(\phi + \frac{a_1\tau}{a_0}\right)C^*, \lambda_3 = -a_0 < 0, \lambda_4 = -b_0 < 0, \lambda_5 = -m_0 < 0.$$

The eigenvalues obtained shows obviously that $\lambda_1, \lambda_3, \lambda_4, \lambda_5$ are real and negative.

For $\lambda_2 = \omega - (\mu_1 + \mu_2) + \left(\phi + \frac{a_1\tau}{a_0}\right)C^*$, we consider two possible cases. The equilibrium point will be locally asymptotically stable (*a sink*) if $\lambda_2 < 0$. That is, when $\omega + \left(\phi + \frac{a_1\tau}{a_0}\right)C^* < (\mu_1 + \mu_2)$. It would be unstable (*a saddle point*) if $\lambda_2 > 0$. That is, when $\omega + \left(\phi + \frac{a_1\tau}{a_0}\right)C^* > (\mu_1 + \mu_2)$.

Hence, the equilibrium point $\varepsilon_1 = (C^*, P^*, R^*, E^*, T^*)$ is locally asymptotically stable if

$$\omega + \left(\phi + \frac{a_1\tau}{a_0}\right)C^* < (\mu_1 + \mu_2) \text{ and unstable if } \omega + \left(\phi + \frac{a_1\tau}{a_0}\right)C^* > (\mu_1 + \mu_2),$$

$$\text{where } C^* = \frac{C_m}{\beta}[\beta - (d_2 + d_3 + d_4 + \mu_0)], \beta > (d_2 + d_3 + d_4 + \mu_0). \quad \square$$

Theorem 3.3. *The equilibrium point $\varepsilon_2 = (C^{**}, P^{**}, R^{**}, E^{**}, T^{**}) = \left(0, \frac{N}{\omega}[\omega - (\mu_1 + \mu_2)], 0, 0, 0\right)$ is locally asymptotically stable if $\beta < (d_1P^{**} + d_2 + d_3 + d_4 + \mu_0)$. It is unstable if $\beta > (d_1P^{**} + d_2 + d_3 + d_4 + \mu_0)$, where $P^{**} = \frac{N}{\omega}[\omega - (\mu_1 + \mu_2)], \omega > (\mu_1 + \mu_2)$.*

Proof. From equation (17), the Jacobian matrix, J_2 , corresponding to the third equilibrium point, $\varepsilon_2 = \left(0, \frac{N}{\omega}[\omega - (\mu_1 + \mu_2)], 0, 0, 0\right)$ is:

$$\begin{vmatrix} \beta - (d_1P^{**} + d_2 + d_3 + d_4 + \mu_0) - \lambda & 0 & 0 & 0 & 0 \\ \phi P^{**} & -\frac{\omega}{N}P^{**} - \lambda & \tau P^{**} & 0 & 0 \\ a_1 & 0 & -a_0 - \lambda & 0 & 0 \\ b_1 & 0 & 0 & -b_0 - \lambda & 0 \\ m_1 & 0 & 0 & 0 & -m_0 - \lambda \end{vmatrix} = 0.$$

On evaluating this determinant, we obtain the following eigenvalues

$$\lambda_1 = \beta - (d_1 P^{**} + d_2 + d_3 + d_4 + \mu_0), \lambda_2 = -\frac{\omega}{N} P^{**} < 0, \lambda_3 = -a_0 < 0, \lambda_4 = -b_0 < 0,$$

$$\lambda_5 = -m_0 < 0.$$

From the evaluation, all eigenvalues except $\lambda_1 = \beta - (d_1 P^{**} + d_2 + d_3 + d_4 + \mu_0)$ are obviously negative. Hence, the equilibrium point, ε_2 , will be locally asymptotically stable (a sink) if $\lambda_1 < 0$ and unstable (a saddle point) if $\lambda_1 > 0$. That is, ε_2 , will be locally asymptotically stable if $\beta < (d_1 P^{**} + d_2 + d_3 + d_4 + \mu_0)$ and unstable if $\beta > (d_1 P^{**} + d_2 + d_3 + d_4 + \mu_0)$, where $P^{**} = \frac{N}{\omega}[\omega - (\mu_1 + \mu_2)]$, $\omega > (\mu_1 + \mu_2)$. \square

Theorem 3.4. *The equilibrium point $\varepsilon_3 = (C^{***}, P^{***}, R^{***}, E^{***}, T^{***})$ is locally asymptotically stable.*

Proof. Substituting $\varepsilon_3 = (C^{***}, P^{***}, R^{***}, E^{***}, T^{***})$ into equation (17), we have:

$$J_3 = \begin{pmatrix} -\frac{\beta}{C_m} C^{***} & -d_1 C & 0 & 0 & 0 \\ \phi P & -\frac{\omega}{N} P^{***} & \tau P^{***} & 0 & 0 \\ a_1 & 0 & -a_0 & 0 & 0 \\ b_1 & 0 & 0 & -b_0 & 0 \\ m_1 & 0 & 0 & 0 & -m_0 \end{pmatrix}.$$

The characteristic equation corresponding to the Jacobian matrix, J_3 , is:

$$\begin{vmatrix} -\frac{\beta}{C_m} C^{***} - \lambda & -d_1 C & 0 & 0 & 0 \\ \phi P & -\frac{\omega}{N} P^{***} - \lambda & \tau P^{***} & 0 & 0 \\ a_1 & 0 & -a_0 - \lambda & 0 & 0 \\ b_1 & 0 & 0 & -b_0 - \lambda & 0 \\ m_1 & 0 & 0 & 0 & -m_0 - \lambda \end{vmatrix} = 0.$$

$$\therefore \lambda_1 = -\frac{\beta}{C_m} C^{***} < 0, \lambda_2 = -\frac{\omega}{N} P^{***} < 0, \lambda_3 = -a_0 < 0, \lambda_4 = -b_0 < 0, \lambda_5 = -m_0 < 0.$$

Since all the eigenvalues are real and negative, the equilibrium point $\varepsilon_3 = (C^{***}, P^{***}, R^{***}, E^{***}, T^{***})$ is locally asymptotically stable. \square

3.4. Parameters and their Values. The following parameter values were used to calculate the concentration number, equilibrium points, sensitivity indices and numerical simulation of the formulated model.

TABLE 2. Values of Model Parameters

Parameters	Values	Units	References
β	1 and 6	$\mu\text{mol per mol } m^{-2}$	[19], [7]
C_m	25	m^{-2}	Fixed
d_1	0.05	m^{-2}	[18]
d_2	0.013	m^{-2}	Fixed
d_3	0.01	m^{-2}	Fixed
d_4	0.5	m^{-2}	[28]
μ_0	0.016	year^{-1}	Fixed
ω	0.8 and 1.0	year^{-1}	[18], [17],[7]
N	80	$\text{kg } m^{-2}$	[17]
ϕ	0.1	m^{-2}	[18]
τ	0.03	m^{-2}	[18]
μ_1	0.02	year^{-1}	[7]
μ_2	0.04	year^{-1}	[17]
a_1	0.008	m^{-2}	Assumed
a_0	0.001	m^{-2}	Assumed
b_1	0.0078	m^{-2}	Assumed
b_0	0.0019	m^{-2}	Assumed
m_1	0.0068	m^{-2}	Assumed
m_0	0.0012	m^{-2}	Assumed

3.5. Sensitivity Analysis. Sensitivity analysis reveals how important each parameter in a formulated model is in the description of such a model. The relevance of the information from it helps in experimental designs, data assimilation and reduction in complexity of nonlinear models [29]. Here, we performed sensitivity analysis on the concentration number, C_* got in equation (16), to determine the influence of each parameter on the dynamics of the formulated model and those that have higher impact on climate change due to excessive CO_2 emission. The results revealed the parameters that would aid the choice of the best mitigation measure(s) to adopt in combating excessive emission and accumulation of CO_2 in the atmosphere.

The normalized forward sensitivity index (NFSI) denoted by say, Ψ , of a variable say, Θ , with respect to a parameter say, π , is the ratio of the relative change in Θ to the relative change in π [29]. If Θ is differentiable with respect to π , the NFSI is defined mathematically as

$$(18) \quad \Psi_{\pi}^{\Theta} = \frac{\partial \Theta}{\partial \pi} \cdot \frac{\pi}{\Theta}.$$

Results of the sensitivity analysis on each parameter of the concentration number(C_*) using the above NFSI formula and the parameter values in Table (2) are presented in Table (3).

TABLE 3. **Sensitivity Indices for the Model using the Concentration Number**

Parameters	Descriptions	Sensitivity Indices
β	Intrinsic rate of accumulation of CO_2 in the atmosphere	0.09870
C_m	Maximum tolerated concentration of CO_2 beyond which the model becomes meaningless	1.00000
d_2	Rate of decrease in CO_2 concentration due to implementation of recycling and good conservation policies	-0.00238
d_3	Rate of decrease in CO_2 concentration due to implementation of enlightenment programmes	-0.00183
d_4	Rate of decrease in CO_2 concentration due to implementation of direct air capture technology	-0.09156
μ_0	Natural rate of depletion in concentration of CO_2	-0.00293
ω	Intrinsic rate of growth of the photosynthetic biomass	-1.06383
ϕ	Rate of increase in the photosynthetic biomass due to the interaction between this biomass and CO_2	1.00000
μ_1	Rate of decrease in photosynthetic biomass due to natural phenomena	0.02128
μ_2	Rate of decrease in photosynthetic biomass due to human activities	0.04255

From the sensitivity analysis carried out using the parameter values in Table (2), we obtained the indices to be either positive or negative (Table 3). From the results presented in Table (3), parameters with positive indices will immensely influence the dynamics of climate change due

to excessive emission negatively as their values increase. C_* will increase as the values of these positive parameters increase and that means more concentration of CO_2 in the atmosphere. The parameters with negative indices will help in minimizing the impact of climate change as their values increase. The parameters with positive indices when decreased would correspondingly reduce the excess concentration of CO_2 in the atmosphere. In same vein, parameters with negative indices when increased would reduce also the excessive emission and accumulation of CO_2 in the atmosphere. For instance, by separately reducing the accumulation rate of CO_2 , β , by 15% and increasing the intrinsic growth rate of the photosynthetic biomass, ω , by 18% would lead to a reduction of about 1.7% and 16.07% in the concentration number respectively. These reductions represent a decrease in the value of excessive concentration of CO_2 in the atmosphere. Combining the effects of the 15% and 18% reduction in the accumulation rate of CO_2 and intrinsic growth rate of the photosynthetic biomass simultaneously would lead to a decrease of about 17.54% in the concentration number which in turn represents a proportionate reduction in the concentration of CO_2 in the atmosphere. Hence, the significance of the results obtained from the analysis is that mitigation measures should be targeted on the most sensitive parameters such as the accumulation rate of CO_2 , β , and the intrinsic growth rate of the photosynthetic biomass, ω , in providing solution to reducing and possibly, removing totally the excessive concentration of CO_2 from the atmosphere.

4. NUMERICAL SIMULATIONS

The numerical simulation is performed to support the results of theoretical analysis and also present further discussions of the dynamics of the model system given by equations (1) to (5). Using the parameter values in Table (2), the four equilibrium points for the model were calculated as:

$$\epsilon_0 = (C^0, P^0, R^0, E^0, T^0) = (0, 0, 0, 0, 0),$$

$$\epsilon_1 = (C^*, P^*, R^*, E^*, T^*) = (22.754, 0, 182.033, 93.412, 128.940),$$

$$\epsilon_2 = (C^{**}, P^{**}, R^{**}, E^{**}, T^{**}) = (0, 75.2, 0, 0, 0),$$

$$\epsilon_3 = (C^{***}, P^{***}, R^{***}, E^{***}, T^{***}) = (1.29, 101, 10.30, 5.28, 7.29).$$

The sensitivity analysis performed on the Concentration Number, C_* , revealed crucial parameters that would help in reducing the accumulated emitted CO_2 in the atmosphere. The numerical

simulation of the model was done using Matlab version R2013b software. Using the parameter values in Table (2) and the inbuilt solver, ode45 (operates based on 5th order Runge-Kutta method), the results given by Table (4) and Figures (1) to (12) were obtained. We note that the infinity value recorded for time taken to reach minimum excessive concentration of CO_2 in Table (4) means that the expected time is out of the range of the chosen time interval plotted ($0 \leq t \leq 10$).

TABLE 4. Summary of Simulation Results for Excessive Concentration of CO_2

Figure	Colour	H_1	H_2	H_3	H_4	$H_5(\%)$
1	magenta (baseline)	1.3748	4.3810	-7.8268×10^{-8}	9.7230	—
	green	2.7461	4.3560	-3.0286×10^{-8}	9.7520	—
	blue	4.4508	4.9680	3.9366×10^{-7}	10	—
2	magenta (baseline)	—	—	—	—	—
	green	0.4054	2.3600	-1.1104×10^{-6}	9.7060	—
	blue	2.7461	4.3560	-3.0286×10^{-8}	9.7520	—
3	magenta (baseline)	24.2496	1.6970	0.1000	∞	—
	green	21.0144	2.6780	0.0056	10	13.34
	blue	10.9094	4.0660	5.2484×10^{-5}	10	55.01
4	magenta (baseline)	23.8666	1.6220	2.1186×10^{-5}	10	—
	green	14.5639	1.6540	-1.1270×10^{-6}	9.7080	38.98
	blue	9.7791	1.6650	-1.1099×10^{-6}	8.6320	59.03
5	magenta (baseline)	24.2496	1.6970	0.1000	∞	—
	green	21.2067	1.3480	-5.1808×10^{-7}	8.1670	12.55
	blue	16.2311	1.1600	-1.1254×10^{-6}	6.4950	33.07
6	magenta (baseline)	24.2496	1.6970	0.1000	∞	—
	green	21.2462	1.3500	-4.8693×10^{-7}	8.2910	12.39
	blue	16.2976	1.1620	-1.1894×10^{-6}	8.3670	32.79

7	magenta (baseline)	24.2496	1.6970	0.1000	∞	—
	green	21.2750	1.3520	-4.6332×10^{-7}	8.3860	12.27
	blue	16.3638	1.1640	-1.1631×10^{-6}	8.4510	32.52
8	magenta (baseline)	24.2496	1.6970	0.1000	∞	—
	green	21.3140	1.3540	-4.3013×10^{-7}	8.5200	12.11
	blue	16.4299	1.1660	-1.1310×10^{-6}	8.5370	32.25
9	magenta (baseline)	24.1919	1.6990	0.1000	∞	—
	green	20.9186	1.3680	-5.0606×10^{-74}	8.3910	13.53
	blue	14.9030	1.1900	-1.2000×10^{-6}	6.6560	35.46
10	magenta (baseline)	24.1497	1.7010	0.1000	∞	—
	green	20.6043	1.3800	-5.5304×10^{-74}	8.3720	14.68
	blue	14.9030	1.2140	-1.1241×10^{-6}	5.3660	38.29
11	magenta (baseline)	22.0348	1.8140	0.1000	∞	—
	green	17.5732	1.5080	-1.1834×10^{-64}	6.2620	20.25
	blue	11.1521	1.3530	-1.1980×10^{-6}	6.7000	49.39
12	magenta (baseline)	—	—	—	—	—
	green	0.1000	0	-1.0418×10^{-6}	9.0020	—
	blue	0.3830	3.9980	-1.0823×10^{-7}	19.5070	—

H_1 : Maximum Excessive Concentration of CO_2

H_2 : Time Taken to Reach Maximum Excessive Concentration of CO_2

H_3 : Minimum Excessive Concentration of CO_2

H_4 : Time Taken to Reach Minimum Excessive Concentration of CO_2

H_5 : Percentage Change in Maximum Excessive Concentration of CO_2

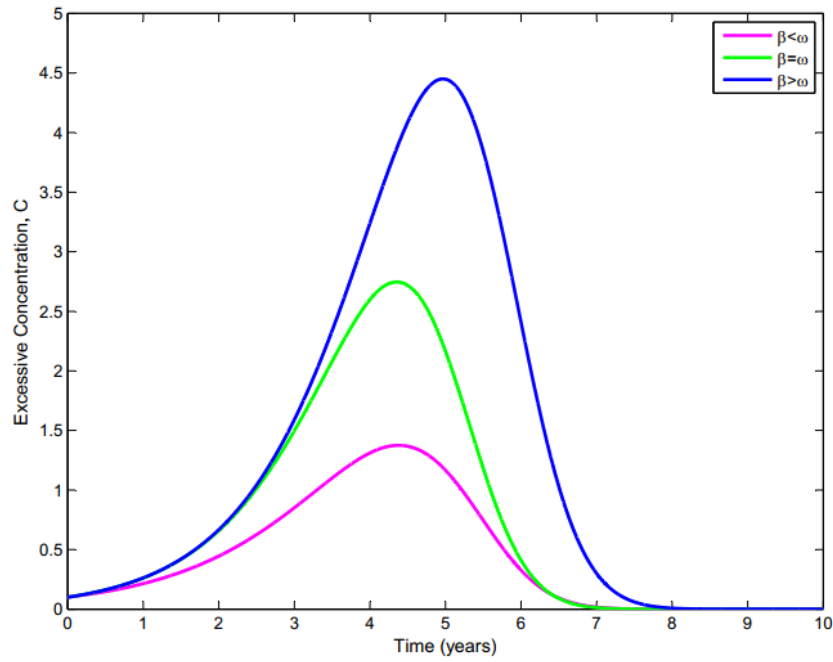


FIGURE 1. Effect of comparing accumulation rate of CO_2 with intrinsic growth rate of photosynthetic biomass

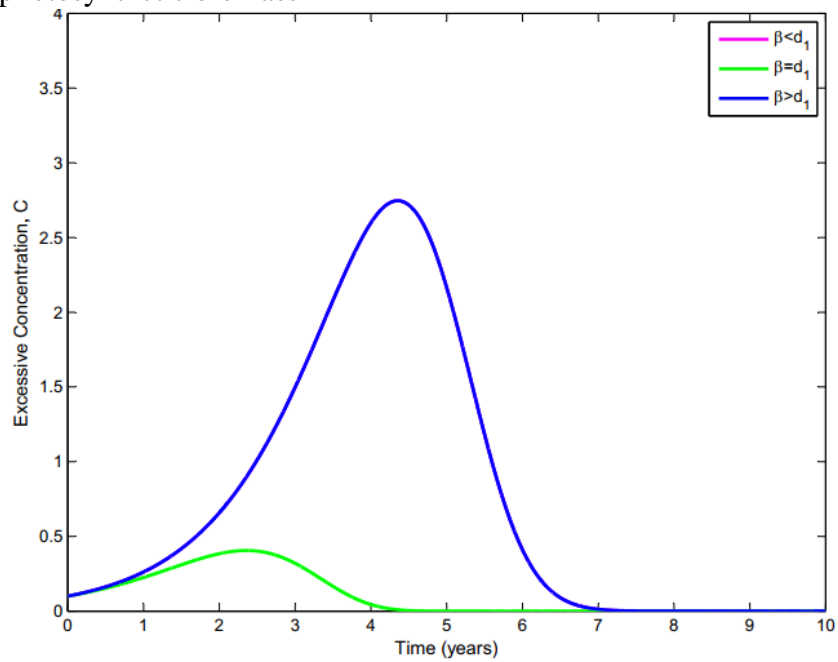
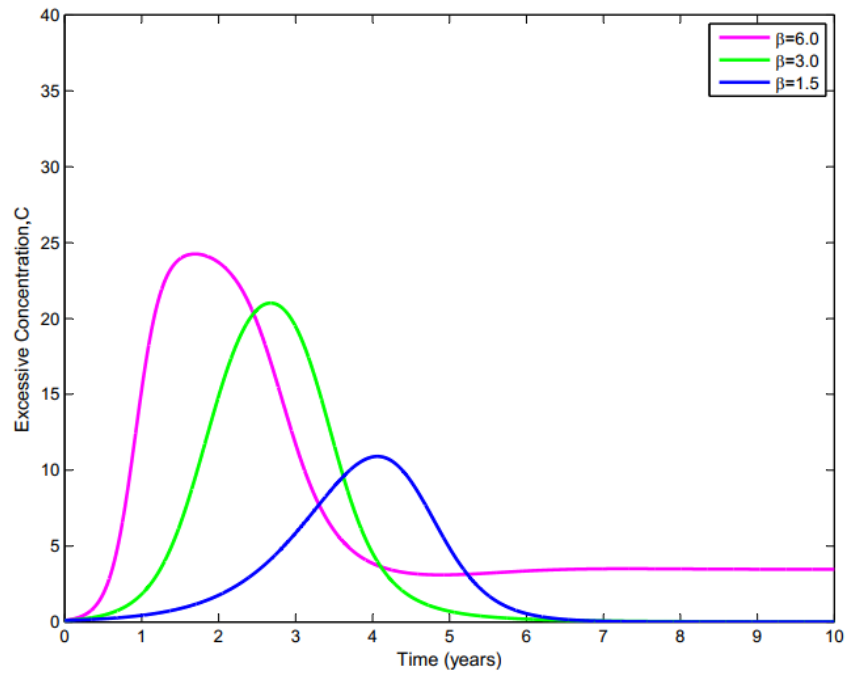
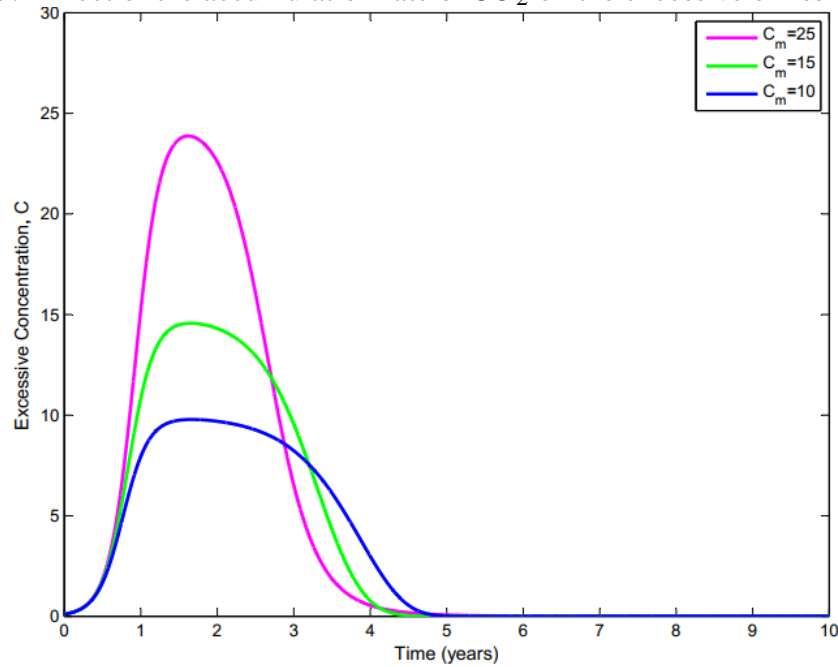


FIGURE 2. Effect of comparing the accumulation rate of CO_2 with the reduction rate of CO_2 by photosynthetic biomass

FIGURE 3. Effect of the accumulation rate of CO_2 on the excessive emission of CO_2 FIGURE 4. Effect of variation of maximum tolerated concentration of CO_2 on the excessive concentration of CO_2

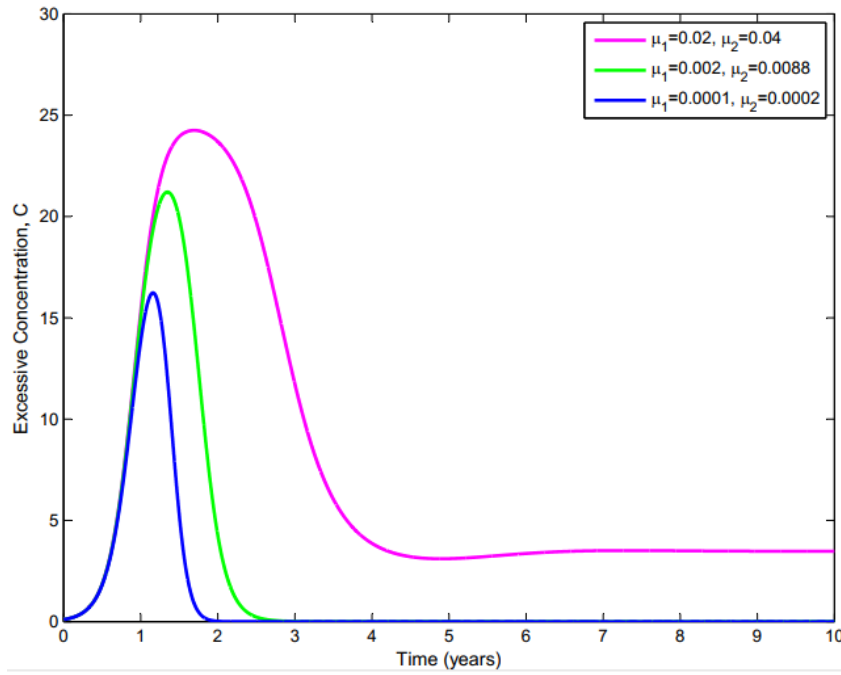


FIGURE 5. Effect of the natural and artificial depletion rates of the photosynthetic biomass on the excessive concentration of CO_2

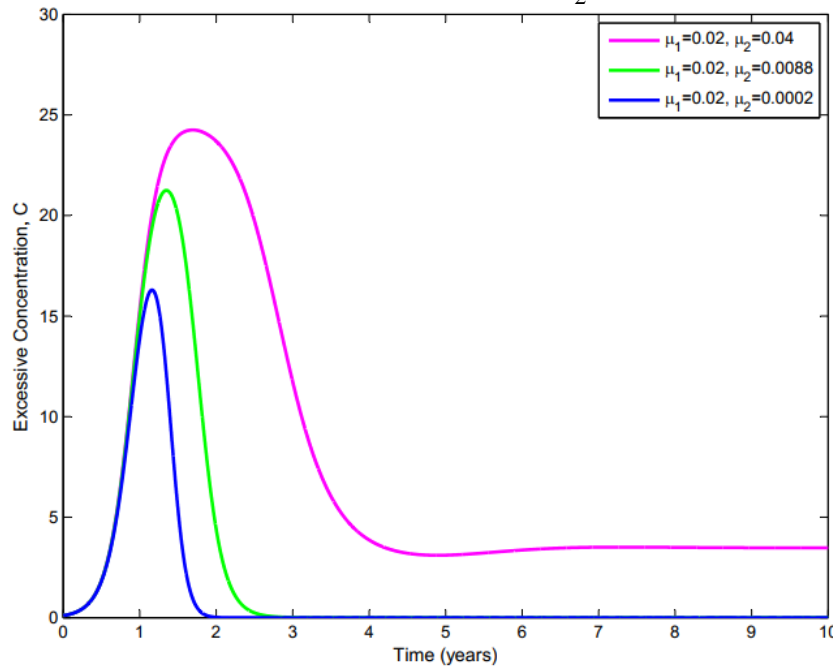


FIGURE 6. Effect of only the artificial depletion rate of the photosynthetic biomass on excessive concentration of CO_2

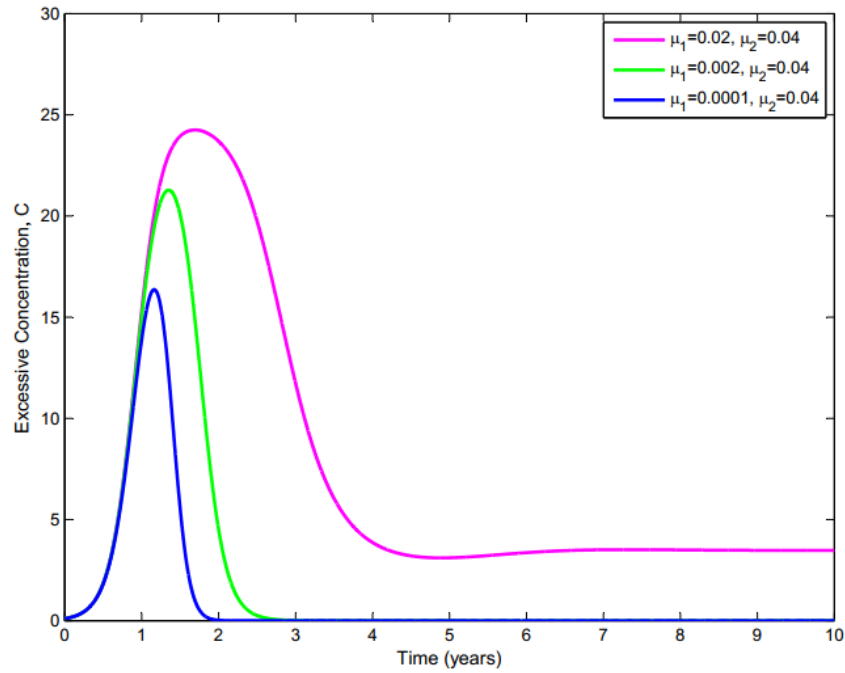


FIGURE 7. Effect of only the natural depletion rate of the photosynthetic biomass on excessive concentration of CO_2

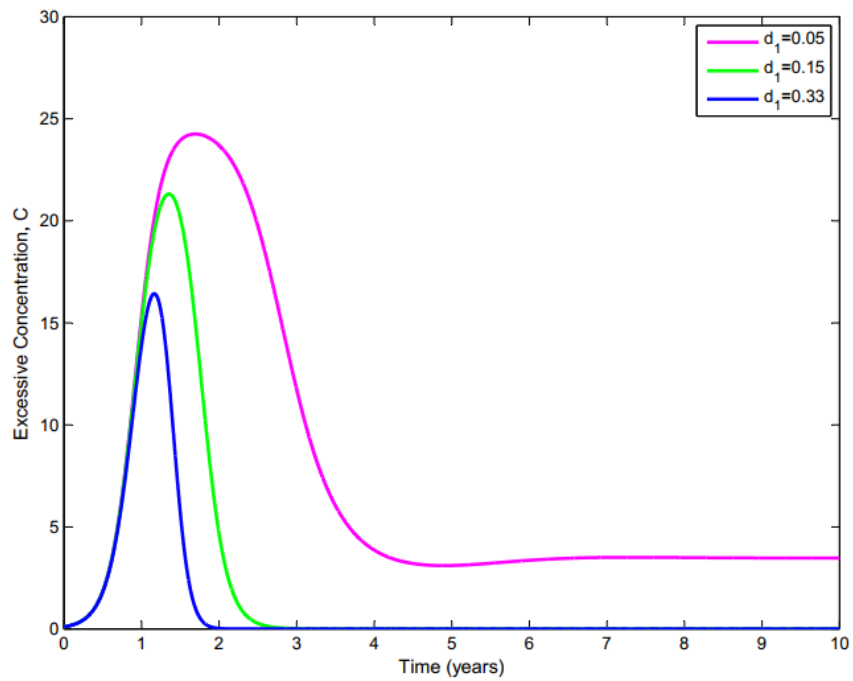


FIGURE 8. Effect of the reduction rate of CO_2 by photosynthetic biomass on excessive concentration of CO_2

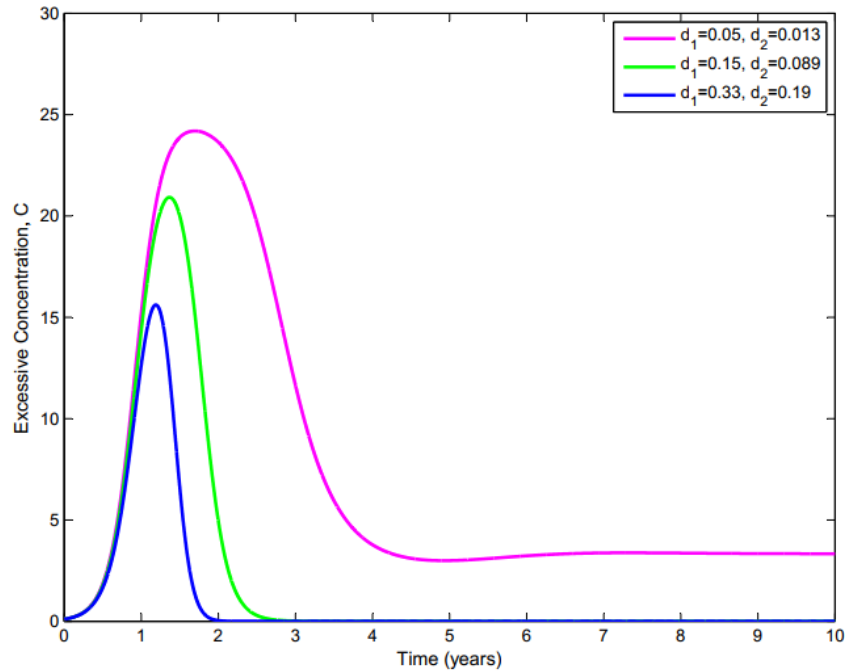


FIGURE 9. Effect of rates of reduction of CO_2 by photosynthetic biomass and good conservation policies on excessive concentration of CO_2

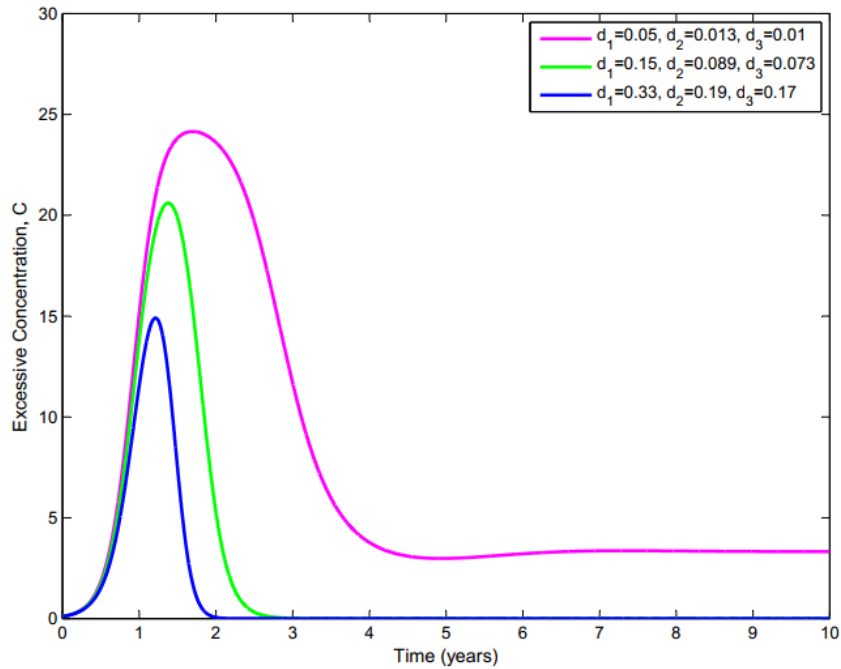


FIGURE 10. Effect of rates of reduction of CO_2 by photosynthetic biomass, good conservation policies and enlightenment programmes on excessive concentration of CO_2

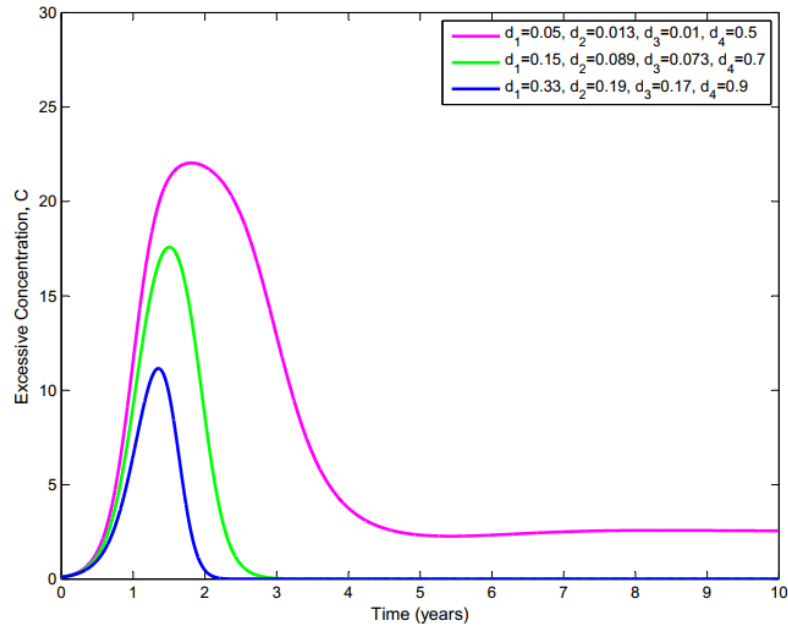


FIGURE 11. Effect of rates of reduction of CO_2 by photosynthetic biomass, good conservation policies, enlightenment programmes and direct air capture technology on excessive concentration of CO_2

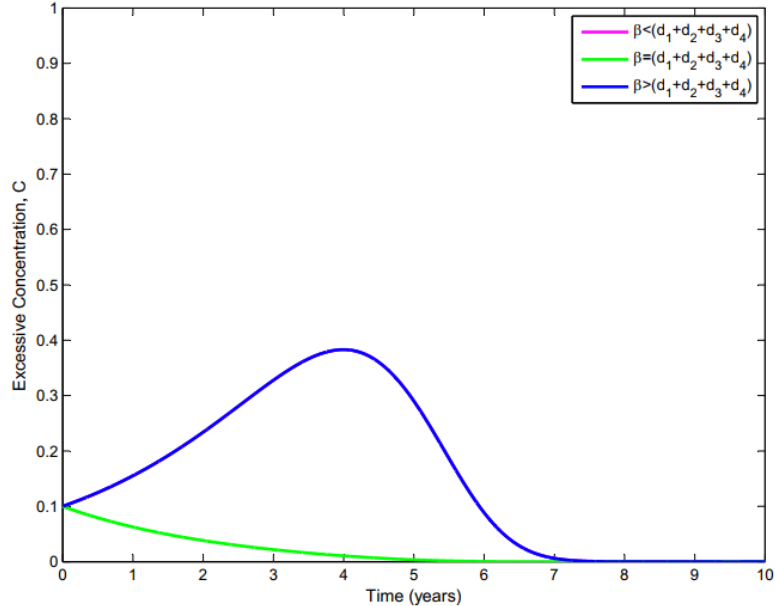


FIGURE 12. Effect of comparing the accumulation rate of CO_2 with combined proportions of success of photosynthetic biomass, good conservation policies, enlightenment programmes and direct air capture technology on excessive concentration of CO_2

The excessive concentration of CO_2 in the atmosphere is dangerous and could pose some threats which could manifest in form of environmental phenomena like flooding, drought, wildlife migration, disease outbreak and many others. In Figure (1), three different hypothetical scenarios between the accumulation rate of CO_2 , β , and the intrinsic growth rate of the photosynthetic biomass, ω are simulated. The least value of the maximum excessive concentration of CO_2 (1.3748) was obtained when the rate of accumulation, β , is less than the intrinsic growth rate of the photosynthetic biomass. This scenario could solely be because adequate attention was paid to conserving and increasing the growth of the photosynthetic biomass which in turn led to more removal of the excessive concentration of CO_2 from the atmosphere. If the rate of increase in the photosynthetic biomass could effectively be maintained and sustained, it would lead to a great reduction of the excess CO_2 and possibly its total removal from the atmosphere. The second scenario shows a moderate value for the maximum excessive concentration of CO_2 (2.7461) when the rate of accumulation of CO_2 is equal to the intrinsic growth rate of the photosynthetic biomass. But the highest value for the maximum excessive concentration of CO_2 (4.4508) was obtained when the accumulation rate of CO_2 was more than the intrinsic growth rate of the photosynthetic biomass. This result is to be expected and aligns with a common reasoning that density of available photosynthetic biomass is overwhelmed in the job of sequestering CO_2 from the atmosphere. Hence, the reason for the highest value compared to the other two earlier scenarios. Therefore, if this be the case, other mitigation measures may be needed in conjunction with the photosynthetic biomass (the natural regulator of CO_2) to help in curbing this excessive concentration that could cause other environmental hazards.

In Figure (2), the results obtained showed that when the accumulation rate was less than the reduction rate of CO_2 by the photosynthetic biomass, there was barely no excessive concentration of carbon CO_2 in the atmosphere to be removed (as seen by the absence of the line for $\beta < d_1$ in Figure (2)). This could be because the photosynthetic biomass has to remove any surplus concentration of CO_2 in the atmosphere due to their high density. When the two rates were equal (accumulation and reduction by photosynthetic biomass rates), we obtained a lower value for the maximum excessive concentration of CO_2 (0.4054). However, when the accumulation rate was higher than the reduction rate of CO_2 by the photosynthetic biomass, we got a very high

value for the maximum excessive concentration of CO_2 (2.7461). This is about 6 times higher than the previous value of 0.4054. This situation reflects reality as the density of photosynthetic biomass available may not be enough to remove the excess accumulated concentration of CO_2 from the atmosphere. Hence, other mitigation measures are required.

In Figure(3), an emission rate of $\beta = 6$ led to an accumulation of CO_2 to a maximum concentration of about 24.2496 in 1.697 years and a corresponding minimum of 0.1000 in a long number of years. Reducing this emission rate to $\beta = 3$ and $\beta = 1.5$ led to maximum concentration values of 21.0144 and 10.9094 in 2.6780 and 4.0660 years respectively. These two values of the maximum concentration of CO_2 are lower and better than the initial base value (24.2496). These values also took longer to attain (2.6780 and 4.0660 years respectively) than the initial base year value (1.6970 years). The reduction in the emission and accumulation rate of CO_2 to $\beta = 3$ and $\beta = 1.5$ also led to minimum concentration values of 0.0056 and 5.2484×10^{-5} respectively in 10 years. These values are also lower than the base minimum concentration value (0.1000) and also took lower duration 10 years to attain than the base value. This reduction in the emission rate of CO_2 can be brought about by efficient and conscious efforts towards checking many activities that contribute to this emission and accumulation while seeking and adopting friendly alternatives to these activities that contribute to this emission. A reduction of the emission rate to $\beta = 3$ and $\beta = 1.5$ led to a reduction of the maximum concentration of CO_2 to 13.34% and 55.01% respectively.

Figure (4) shows the effect of variation of the maximum tolerated concentration of CO_2 , C_m , on the excessive emitted and accumulated concentration of CO_2 in the atmosphere. Effective implementation of a number of measures would lead to a reduction in the maximum tolerated concentration of CO_2 . As presented in Figure (4), decreasing the maximum tolerated concentration from $C_m = 25$ to $C_m = 15$ and $C_m = 10$ correspondingly led to reduction in the maximum excessive concentration of CO_2 from 23.8666 to 14.5639 and 9.7791 respectively. These reduced values are equivalent to about 38.98% and 59.03% reduction in the maximum excessive concentration of CO_2 in the atmosphere.

Figure (5) shows the effect of varying both the natural and artificial depletion rates of the photosynthetic biomass simultaneously on the dynamics of reduction of excessive concentration

of CO_2 in the atmosphere. Combined base values of both rates, $\mu_1 = 0.02$ and $\mu_2 = 0.04$, gave a maximum concentration value of 24.2496. A simultaneous reduction in both rates to $\mu_1 = 0.002, \mu_2 = 0.0088$ and $\mu_1 = 0.0001, \mu_2 = 0.0002$ resulted in lower maximum concentration values of 21.2067 and 16.2311 respectively. These values respectively depict 12.55% and 33.07% reduction in the maximum excessive concentration of CO_2 in the atmosphere.

In Figure (6), the effect of the variation of the artificial depletion rate of the photosynthetic biomass on the dynamics of reduction of excessive emission and accumulation of CO_2 in the atmosphere is depicted. The artificial depletion of the photosynthetic biomass is mainly by deforestation and bush fires. By keeping the natural death rate of the photosynthetic biomass constant and varying the artificial destruction rate, an initial (baseline) artificial depletion rate of $\mu_2 = 0.04$ produced a maximum excessive concentration value of 24.2496. By reducing this artificial rate to $\mu_2 = 0.0088$ and $\mu_2 = 0.0002$, we obtained lower maximum excessive concentration values of 21.2462 and 16.2976 respectively. These lower values correspond respectively to 12.39% and 32.79% reduction in the maximum excessive concentration of CO_2 .

In Figure (7), the effect of variation of natural death rate of the photosynthetic biomass, μ_1 , in the reduction of excessive emission and accumulation of CO_2 in the atmosphere while keeping the artificial depletion rate constant are plotted. There are many natural phenomena and activities that can increase the natural depletion of the photosynthetic biomass such as disease outbreak, pest infestation, overgrazing, flooding, drought and many others. If these activities can be put under check, it could lead to a reduction in the natural depletion of the photosynthetic biomass. This is evident in the results got as shown in Figure(7). A natural depletion rate of the photosynthetic biomass of $\mu_1 = 0.02$ produced a maximum excessive concentration value of 24.2496. But a reduction in value of this rate to $\mu_1 = 0.002$ and $\mu_1 = 0.0001$ gave lower concentration values of 21.2750 and 16.3638 respectively. These respective concentration values are equivalent to 12.27% and 32.52% reduction in the maximum excessive concentration of CO_2 in the atmosphere respectively.

The natural mechanism in place to remove CO_2 from the atmosphere is the anabolic process called photosynthesis, through which 'chlorophyllic' biomass (photosynthetic biomass) manufacture food to sustain the ecosystem. But due to increased human population that leads to

further quest for survival, accommodation, industrialization, urbanization and others, the natural system in place is overwhelmed. Forests are destroyed in search of many products and this lead to a reduction in the photosynthetic biomass density. By engaging in good conservation practices like reforestation, afforestation and minimizing excessive and uncontrolled destruction of the photosynthetic biomass, we could increase greatly the photosynthetic biomass density which in turn would contribute to reducing this excessive emitted and accumulated concentration of CO_2 in the atmosphere. This is evident in Figure (8) from the simulation results obtained. Initially, the inadequate photosynthetic biomass density led to a maximum excessive concentration of 24.2496 in 1.6970 years. But increasing the rate from $d_1 = 0.05$ to $d_1 = 0.15$ and $d_1 = 0.33$ led to maximum excessive concentration values of 21.3140 and 16.4299 and corresponding minimum excessive concentration values of -4.3013×10^{-7} and -1.1310×10^{-6} respectively. These values are lower than the initial maximum and minimum excessive concentration values of 24.2496 and 0.1000 respectively that correspond to $d_1 = 0.05$. These results imply that if we can put in some effort in increasing the photosynthetic biomass density, we can reduce the excessive emission and accumulation of CO_2 in the atmosphere by 12.11% and 32.25% respectively as seen in Table (4).

The photosynthetic biomass alone may not have the capacity to effectively remove the excessive emitted and accumulated concentration of CO_2 from the atmosphere within a relatively short period of time. Hence, we need other mitigation measures such as good conservation policies, enlightenment programmes and direct air capture technology to support the natural mechanism of photosynthetic biomass.

In Figure (9), we simulated the effect of combining rates of good conservation policies and the photosynthetic biomass in reducing the excess CO_2 in the atmosphere. The initial simulation result of 24.1919 for maximum excessive concentration of CO_2 is better than the initial result of 24.2496 obtained for photosynthetic biomass only. Improving the two rates (d_1 and d_2) associated with these two measures led to percentage reductions of about 13.53% and 35.46% respectively (as seen in Table (4)).

In Figure (10), the effect of combining photosynthetic biomass, good conservation policies and enlightenment programmes rates in reducing the excessive concentration of CO_2 in the

atmosphere are displayed. The simulation baseline result of 24.1497 for maximum excessive concentration of CO_2 is an improved result compared to the previous results of 24.1919 (for a combination of photosynthetic biomass and good conservation policies only) and 24.2496 (for photosynthetic biomass only). Improvement in the effective combination of these three measures (photosynthetic biomass, good conservation policies and enlightenment programmes only) led to about 14.68% and 38.29% reduction in the maximum excessive concentration of CO_2 .

In Figure (11), the results of combining rates of photosynthetic biomass, good conservation policies, enlightenment programmes and direct air capture technology in the dynamics for the reduction of the excessive concentration CO_2 in the atmosphere are presented. The initial simulation result for the excessive concentration of CO_2 of about 22.0348 is better than the other initial maximum excessive concentrations (24.2496, 24.1919 and 24.1497 respectively) obtained earlier. This combination of all the four measures led to about 20.25% and 49.39% reduction in the maximum excessive concentration of CO_2 in the atmosphere.

In Figure (12), comparison of different cases between the accumulation rate of CO_2 , β , and the combined rates of photosynthetic biomass, good conservation policies, enlightenment programmes and direct air capture technology are shown. When the accumulation rate was less than these combined rates from all the mitigation measures, the excessive concentration was removed and hence, the reason there is no line in Figure (12) to depict this particular scenario. When the accumulation rate of CO_2 was equal to the combined rates of the mitigation measures, we got a maximum excessive concentration value of about 0.1000. But for the situation where the accumulation rate was higher than the combined rates of all the measures, we got a higher maximum excessive concentration of 0.3830 which is about 3 times higher than the previous value of 0.1000.

5. CONCLUSION

In this research paper, we focused our attention on carbon dioxide which is the most vital greenhouse gas that contributes to the recent global warming. We developed a five compartment deterministic nonlinear mathematical model to study this problem of climate change due to excessive emission and accumulation of carbon dioxide. In the mathematical analysis of the

model, four equilibrium points were obtained. The local stability analysis of each of the equilibrium points was done. Using the idea of the next generation matrix (NGM), a novel threshold quantity called Concentration Number was derived. For our developed model, we obtained the concentration number to be 2.4207 using the parameter values given in Table(2). Since this value is greater than one, it means the excessive concentration of this gas could pose a potential threat to the environment. Hence, other mitigation measures were needed. The sensitivity analysis on the concentration number was done using the normalized forward sensitivity index (NFSI) method. The results revealed the most crucial parameters that influenced the dynamics of the model such as the accumulation rate of carbon dioxide, intrinsic growth rate of the photosynthetic biomass and others. These results also influenced and informed the choice of parameters varied in the simulation of the model.

The numerical simulation of the model was done using MATLAB R2013b software. Many influential parameters identified by carrying out sensitivity analysis were varied during the simulation of the model. A summary of the findings from the simulation results showed that the excessive and accumulated concentration of CO_2 in the atmosphere can be reduced.

DATA AVAILABILITY

The data used in the numerical simulations and other calculations in this study were got from research materials whose sources are appropriately cited as seen in Table (2) while others were fixed or assumed.

ACKNOWLEDGEMENT

The corresponding author on behalf of the authors is grateful to the African Union Commission for her financial assistance and sponsorship to study under her Pan African University Scholarship Scheme in Pan African University Institute of Basic Sciences, Technology and Innovation (PAUISTI).

CONFLICT OF INTERESTS

The author(s) declare that there is no conflict of interests.

REFERENCES

- [1] M. Ba-Shammakh, An optimization approach for integrating planning and carbon dioxide mitigation in the power and refinery sectors, Ph.D. thesis, University of Waterloo, Canada. (2007).
- [2] P. Zhu, W. Xie, Y. Shi, et al. Forecasting carbon dioxide emissions using a novel conformable fractional order discrete grey model, preprint, (2021). <https://doi.org/10.21203/rs.3.rs-809289/v1>.
- [3] A.K. de Souza Mendonça, S.A. da Silva, L.Z. Pereira, et al. An overview of environmental policies for mitigation and adaptation to climate change and application of multilevel regression analysis to investigate the CO₂ emissions over the years of 1970 to 2018 in all Brazilian states, *Sustainability*. 12 (2020), 9175. <https://doi.org/10.3390/su12219175>.
- [4] P. Kumar, V. Govindaraj, V.S. Erturk, et al. Effects of greenhouse gases and hypoxia on the population of aquatic species: a fractional mathematical model, *Adv. Contin. Discr. Models*. 2022 (2022), 31. <https://doi.org/10.1186/s13662-022-03679-8>.
- [5] S. Mandal, M.S. Islam, S. Akter, et al. A mathematical model to investigate the frequent impact of global warming on coastal lives, in: *Proceedings of the International Conference on Industrial and Mechanical Engineering and Operations Management*, Dhaka, Bangladesh, 2020.
- [6] M.H.A. Biswas, P.R. Dey, M.S. Islam, et al. Mathematical Model Applied to Green Building Concept for Sustainable Cities Under Climate Change, *J. Contemp. Urban Aff.* 6 (2021), 36-50. <https://doi.org/10.25034/ijcua.2022.v6n1-4>.
- [7] P. Panja, Is the forest biomass a key regulator of global warming?: A mathematical modelling study, *Geol. Ecol. Landscapes*. 6 (2020), 66-74. <https://doi.org/10.1080/24749508.2020.1752021>.
- [8] M.A.L. Caetano, D.F.M. Gherardi, G. de P. Ribeiro, et al. Reduction of CO₂ emission by optimally tracking a pre-defined target, *Ecol. Model.* 220 (2009), 2536-2542. <https://doi.org/10.1016/j.ecolmodel.2009.06.003>.
- [9] A.K. Misra, M. Verma, E. Venturino, Modeling the control of atmospheric carbon dioxide through reforestation: effect of time delay, *Model. Earth Syst. Environ.* 1 (2015), 24. <https://doi.org/10.1007/s40808-015-0028-z>.
- [10] S. Sundar, An ecological type nonlinear model for the removal of carbon dioxide from the atmosphere by introducing liquid species, *Comb. Ecol. Softw.* 3 (2013), 33-43.
- [11] E. Specht, T. Redemann, N. Lorenz, Simplified mathematical model for calculating global warming through anthropogenic CO₂, *Int. J. Thermal Sci.* 102 (2016), 1-8. <https://doi.org/10.1016/j.ijthermalsci.2015.10.039>.
- [12] N. Jaoua, Mathematical model for CO₂ emissions reduction to slow and reverse global warming, in: J. P. Tiefenbacher (Ed.), *Global Warming and Climate Change*, IntechOpen, 2020. <https://doi.org/10.5772/intechopen.88961>.

- [13] M.A.L. Caetano, D.F.M. Gherardi, T. Yoneyama, An optimized policy for the reduction of CO₂ emission in the Brazilian Legal Amazon, *Ecol. Model.* 222 (2011), 2835-2840. <https://doi.org/10.1016/j.ecolmodel.2011.05.003>.
- [14] J.B. Shukla, A.K. Mishra, S. Sundar, et al. Modeling the removal of carbon dioxide from the atmosphere by spraying external species above the sources of emissions: A mechanism to reduce global warming, *Int. e-J. Math. Model. Anal. Complex Syst.: Nat. Soc.* 1 (2015), 7-21.
- [15] M.A. Hesse, Mathematical modeling and multiscale simulation of carbon dioxide storage in saline aquifers, Ph.D. thesis, Stanford University, (2008).
- [16] J.B. Shukla, S. Sundar, A.K. Mishra, et al. Modeling the removal of carbon dioxide from the near earth atmosphere using external species and greenbelts plantation around sources of emissions, *Int. e-J. Math. Model. Anal. Complex Syst.: Nat. Soc.* 1 (2015), 22-35.
- [17] A.H. Teru, P.R. Koya, Mathematical modelling of deforestation of forested area due to lack of awareness of human population and its conservation, *Math. Model. Appl.* 5 (2020), 94-104. <https://doi.org/10.11648/j.mma.20200502.15>.
- [18] K.R. Gandhi, M.R. Tailor, Solution of problems arising due global warming and climate change in the modelling process, *Int. J. Res. Appl. Sci. Eng. Technol.* 8 (2020), 2190-2197.
- [19] B.F. Etin-Osa, I.M. Azubike, Parametric sensitivity analysis of a mathematical model of the effect of carbon dioxide on the climate change, *Appl. Comput. Math.* 9 (2020), 96-101.
- [20] P. van den Driessche, Reproduction numbers of infectious disease models, *Infect. Dis. Model.* 2 (2017), 288-303. <https://doi.org/10.1016/j.idm.2017.06.002>.
- [21] A.F. Bezabih, G.K. Edessa, P.R. Koya, Mathematical eco-epidemiological model on prey-predator system, *Math. Model. Appl.* 5 (2020), 183-190. <https://doi.org/10.11648/j.mma.20200503.17>.
- [22] C. Okoye, O.C. Collins, G.C.E. Mbah, Mathematical approach to the analysis of terrorism dynamics, in: J.T. Omenma, I.E. Onyishi, A.-M. Okolie (Eds.), *Ten Years of Boko Haram in Nigeria*, Springer Nature Switzerland, Cham, 2023: pp. 95-106. https://doi.org/10.1007/978-3-031-22769-1_5.
- [23] P.U. Madueme, V.O. Eze, N.S. Aguegbah, Dynamics of prey predator model with prey refuge using a threshold parameter, *J. Math. Comput. Sci.* 11 (2021), 5937-5946. <https://doi.org/10.28919/jmcs/6184>.
- [24] O.C. Collins, K.J. Duffy, Consumption threshold used to investigate stability and ecological dominance in consumer-resource dynamics, *Ecol. Model.* 319 (2016), 155-162. <https://doi.org/10.1016/j.ecolmodel.2015.03.021>.
- [25] P.G. Madueme, G.C.E. Mbah, Dynamics of interacting species for a consumer resource system, *Int. J. Sci. Eng. Res.* 9 (2018), 167-174.

- [26] P.M. Tchepmo Djomegni, E.F. Doungmo Goufo, S.K. Sahu, M. Mbehou, Coexistence and harvesting control policy in a food chain model with mutual defense of prey, *Nat. Resource Model.* 32 (2019), 1-23. <https://doi.org/10.1111/nrm.12230>.
- [27] K.J. Duffy, O.C. Collins, Consumer-resource coexistence as a means of reducing infectious disease, *J. Biol. Dyn.* 13 (2019), 177-191. <https://doi.org/10.1080/17513758.2019.1577994>.
- [28] A. Altamirano-Fernández, A. Rojas-Palma, S. Espinoza-Meza, Optimal management strategies to maximize carbon capture in forest plantations: a case study with *Pinus radiata* D. Don, *Forests.* 14 (2023), 82. <https://doi.org/10.3390/f14010082>.
- [29] S. Rosa, D.F.M. Torres, Parameter estimation, sensitivity analysis and optimal control of a periodic epidemic model with application to HRSV in Florida, *Statistics, Optim. Inform. Comput.* 6 (2018), 139-149. <https://doi.org/10.19139/soic.v6i1.472>.